8-5-2010

Tunable double negative band structure from non-magnetic coated rods

Yue Chen
Louisiana State University

Robert Lipton
Louisiana State University

Recommended Citation
Chen, Y., & Lipton, R. (2010). Tunable double negative band structure from non-magnetic coated rods. *New Journal of Physics, 12* https://doi.org/10.1088/1367-2630/12/8/083010

OPEN ACCESS

Tunable double negative band structure from non-magnetic coated rods

To cite this article: Yue Chen and Robert Lipton 2010 *New J. Phys.* **12** 083010

New Journal of Physics
The open-access journal for physics

Tunable double negative band structure from non-magnetic coated rods

Yue Chen[1] **and Robert Lipton**[1]
Department of Mathematics, Louisiana State University, Baton Rouge, LA 70803, USA
E-mail: chenyue@math.lsu.edu and lipton@math.lsu.edu

New Journal of Physics **12** (2010) 083010 (14pp)
Received 12 May 2010
Published 5 August 2010
Online at http://www.njp.org/
doi:10.1088/1367-2630/12/8/083010

Abstract. A system of periodic poly-disperse-coated nano-rods is considered. Both the coated nano-rods and the host material are non-magnetic. The exterior nano-coating has a frequency-dependent dielectric constant and the rod has a high dielectric constant. A negative effective magnetic permeability is generated near the Mie resonances of the rods, while the coating generates a negative permittivity through a field resonance controlled by the plasma frequency of the coating and the geometry of the crystal. The explicit band structure for the system is calculated in the subwavelength limit. Tunable pass bands exhibiting negative group velocity are generated and correspond to simultaneously negative effective dielectric permittivity and magnetic permeability. These can be explicitly controlled by adjusting the distance between the rods, the coating thickness and the rod diameters.

Contents

[1] Authors to whom any correspondence should be addressed.

1. Introduction

Metamaterials are a new class of man-made materials that impart unconventional electromagnetic properties derived from subwavelength configurations of different conventional materials [1]. The first such materials were seen to exhibit behavior associated with negative bulk dielectric constant [2] and were constructed from a cubic lattice of metal wires. Subsequently, negative effective magnetic permeability at microwave frequencies [1] was derived from periodic arrays of non-magnetic metallic split-ring resonators [1]. Double negative or left-handed metamaterials with simultaneous negative bulk permeability and permittivity at microwave frequencies have been developed using periodic arrays of metallic posts and split ring resonators [3]. Subsequent work has delivered several new designs using different configurations of metallic resonators for double negative behavior [4]–[12].

For higher frequencies in the infrared and optical range, an alternative strategy for constructing negative effective permeability from non-magnetic components relies on the Mie resonances associated with small rods or particles made from high permittivity materials [13, 14]. A double negative metamaterial may be achieved by coating the high-permittivity material with a metallic coating having a frequency-dependent dielectric constant with plasmonic or Drude-type behavior at optical frequencies [15]–[17].

In this paper, we focus on the second approach and propose periodic assemblages of aligned non-magnetic dielectric rods, each clad with a non-magnetic plasmonic coating. For this case, we are able to explicitly calculate the propagation band structure in the subwavelength limit. The pass bands and stop bands are given by formulae that depend explicitly on the rod diameters and coating thickness. We show how to construct tunable pass bands associated with double negative effective properties. The physical origin of the negative effective permeability is due to the excitations of Mie resonances inside the rods. On the other hand, the negative effective permittivity is caused by the extreme dielectric properties near the plasma resonance of the coating. We provide the explicit relationship linking Mie resonances and the frequency-dependent effective permittivity to the spacing of the rods, the rod radii and the coating thickness for the coated rod assemblage proposed here.

These relationships are found not by appealing to effective medium theory based on the Clausius–Mossotti formula, but instead we show that it is profitable to take a different approach and characterize wave propagation using explicit multiscale expansions for waves inside the metamaterial crystal. The wave number associated with a Bloch wave inside the d-periodic crystal is denoted by $k = 2\pi/\lambda$, where λ is the wavelength. The approach taken here provides an explicit power series expansion for the fields in the parameter $\eta = dk$. We outline a systematic framework in which the homogenized dispersion relation is recovered directly from the expansion in the subwavelength $d \ll \lambda$ limit. We introduce metamaterial crystals made from coated rod assemblages and obtain explicit homogenized dispersion relations for these geometries. The dispersion relations provide explicit conditions on the distance between neighboring rods, rod radii and coating thickness necessary for generating pass bands associated with double negative behavior. Two examples are provided, showing how the band structure can be manipulated to generate double negative pass bands with negative group velocity.

We conclude by referring to related work addressing wave propagation inside high-contrast media. In the case when the crystal period and wavelength have the same length scales, the ability to open band gaps for metamaterial crystals is established and developed in the set of papers [18]–[20]. The power series strategy presented here for subwavelength analysis has

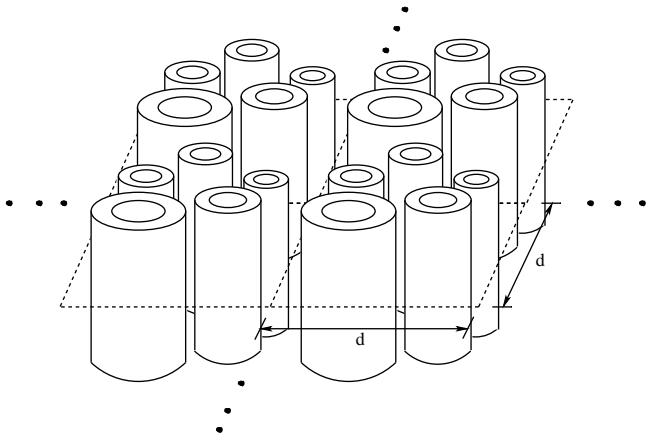

Figure 1. Photonic crystal made from coated rods.

been utilized earlier and developed in [21] for characterizing the dynamic dispersion relations for Bloch waves inside plasmonic crystals and for understanding the influence of effective negative permeability on the propagation of Bloch waves inside high-contrast dielectrics [22]. Earlier work on two-scale homogenization theory for high-contrast dielectrics delivers a frequency-dependent effective magnetic permeability [23]–[25] identical to the generic effective permeability tensor recovered here (see also the work [26] for homogenization in high-contrast media). The connection between high-contrast interfaces, homogenization and the associated generation of negative effective magnetic permeability is established in [27]. An alternative strategy for generating negative permeability at infrared and optical frequencies using special configurations of plasmonic nanoparticles is introduced in [28], and artificial magnetism in periodic metal–dielectric–metal laminates has been investigated in [29]. More recently, two-scale homogenization theory has been developed for three-dimensional (3D) split-ring structures that deliver negative effective magnetic permeability [30, 31] and for metal fibers delivering a negative effective dielectric constant [32]. An analysis of negative refraction and superlensing for split-ring resonators is given in [33], and a method for creating metamaterials with prescribed effective dielectric permittivity and effective magnetic permeability at a fixed frequency is developed in [34].

2. Electromagnetic fields inside metamaterial crystals made from coated rods and the subwavelength limit

The metamaterial is a 2D crystal made of parallel coated rods (see figure 1). There can be one or more coated rods inside the crystal period. The time harmonic field is p-polarized and the magnetic field inside the crystal is $\mathbf{H} = H(\mathbf{x})\exp(-\mathrm{i}\omega t)\mathbf{e}_3$, where $\mathbf{x} = (x_1, x_2)$ in the x_1x_2-plane.

The period for the crystal is d and the dielectric coefficient $\epsilon_{\mathrm{d}}(\mathbf{x})$ takes the values

$$\epsilon_{\mathrm{d}}(\mathbf{x}) = \begin{cases} \epsilon_{\mathrm{R}} & \text{in the rod,} \\ \epsilon_{\mathrm{p}} & \text{in the coating,} \\ \epsilon_{\mathrm{h}} & \text{in the hostmaterial.} \end{cases} \tag{2.1}$$

The coating is a cylindrical shell of plasmonic material with dielectric constant $\epsilon_{\mathrm{p}}(\omega^2/c^2) = 1 - \frac{\omega_{\mathrm{p}}^2/c^2}{\omega^2/c^2}$. Here, ω_{p} is the plasma frequency associated with the coating material and c is the

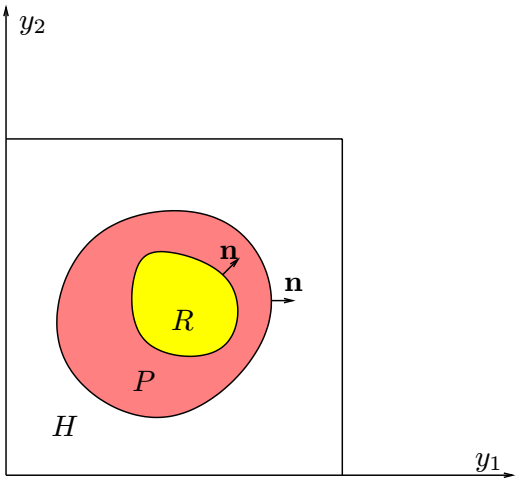

Figure 2. Unit cell containing a single rod cross-section. R represents the rod cross-section, P the plasmonic coating and H the host.

speed of light in vacuum. The dielectric constant of the rod is chosen according to $\epsilon_R = \frac{\epsilon_r}{d^2}$, where ϵ_r has units of area. The idea is to choose the dielectric permittivity of the rod to be large so that the corresponding Mie resonances are excited in the subwavelength limit. The dielectric constant of the host material is given by $\epsilon_h = 1$.

The time harmonic magnetic field for the d-periodic crystal is a Bloch wave,

$$H = h(\mathbf{x}) \exp(\mathrm{i}k\hat{\kappa} \cdot \mathbf{x}), \tag{2.2}$$

where h is d-periodic in $\mathbf{x}$, the wave number is given by k and the direction of propagation in the x_1x_2-plane is described by the unit vector $\hat{\kappa} = (\hat{\kappa}_1, \hat{\kappa}_2)$. H satisfies the Helmholtz equation,

$$\nabla \cdot \epsilon_d^{-1} \nabla H = -\frac{\omega^2}{c^2} H, \tag{2.3}$$

with propagation bands described by dispersion relations involving ω and $k\hat{\kappa}$. We examine the situation in the subwavelength limit when d tends to 0. Instead of developing an effective medium theory based on the Clausius–Mossotti formula, we show that it is profitable to take a different approach and expand the Bloch wave in a multiscale power series in $\eta = kd$. Here, we develop a multiscale power series expansion for h to recover 'homogenized subwavelength' dispersion relations for plane waves inside a magnetically active double negative effective medium.

We introduce the variable $\mathbf{y} = \mathbf{x}/d$ that takes the period cell of size d into the unit period cell Y. Here, Y is split into the subdomains given by the union of rod cross-sections R, the rod coatings P and the host H. Figure 2 illustrates a unit cell Y containing one coated rod cross-section. The expansion parameter is given by $\eta = kd = \frac{2\pi d}{\lambda}$. The subwavelength limit is described by $\eta \to 0$ for a λ fixed. In what follows it is useful to introduce ξ defined by $\xi^2 = \frac{\omega^2}{c^2 k^2}$. The propagation equations satisfied by h for y in the unit period Y are

$$\begin{aligned} -Lh &= \eta^2 \xi^2 h, \text{ in the host,} \\ -Lh &= \eta^2 \xi^2 \epsilon_P(\xi^2 k^2) h, \text{ in the coating,} \\ -Lh &= \epsilon_r \xi^2 k^2 h, \text{ in the rod,} \end{aligned} \tag{2.4}$$

where

$$Lh = \Delta h + 2\mathrm{i}\eta\hat{\kappa}\cdot\nabla h - \eta^2 h, \tag{2.5}$$

$$\epsilon_{\mathrm{P}}(\xi^2 k^2) = 1 - \frac{\omega_{\mathrm{P}}^2/c^2}{\xi^2 k^2}, \tag{2.6}$$

and the transmission conditions

$$n\cdot\left(\nabla h + \mathrm{i}\eta\hat{\kappa}h\right)_{|\mathrm{H}} = n\cdot\epsilon_{\mathrm{P}}^{-1}(\xi^2 k^2)\left(\nabla h + \mathrm{i}\eta\hat{\kappa}h\right)_{|\mathrm{C}},\ \text{H–C interface}, \tag{2.7}$$

$$n\cdot\epsilon_{\mathrm{P}}^{-1}(\xi^2 k^2)\left(\nabla h + \mathrm{i}\eta\hat{\kappa}h\right)_{|\mathrm{C}} = n\cdot\left(\frac{\eta^2}{k^2\epsilon_{\mathrm{r}}}\right)\left(\nabla h + \mathrm{i}\eta\hat{\kappa}h\right)_{|\mathrm{R}},\ \text{R–C interface}. \tag{2.8}$$

Here, the interface separating the host phase and the coating phase is denoted by H–C and the interface between the coating phase and the rod is denoted by R–C. Evaluation of quantities on the host side of the interface is denoted by subscript H, on the coating side by C and on the rod side by R. The unit normal vector n on the host–coating interface points from the coating into the host, and the unit normal vector on the rod–coating interface points from the rod into the coating. We expand h and ξ^2 as

$$h(d\,\mathbf{y}) = h_0(\mathbf{y}) + \eta h_1(\mathbf{y}) + \eta^2 h_2(\mathbf{y}) + \cdots, \tag{2.9}$$

$$\xi^2 = \xi_0^2 + \eta\xi_1^2 + \eta^2\xi_2^2 + \cdots, \tag{2.10}$$

where each term in the expansion is continuous in $\mathbf{y}$ and periodic on Y. Substitution of the expansion into (2.4), (2.7) and (2.8) equating like powers of η gives the following equations used to determine h_0,

$$-\Delta h_0 = 0,\ \text{in the host}, \tag{2.11}$$

$$-\Delta h_0 = 0,\ \text{in the coating}, \tag{2.12}$$

$$-\Delta h_0 = \epsilon_{\mathrm{r}}\xi_0^2 k^2 h,\ \text{in the rod}, \tag{2.13}$$

and transmission conditions

$$n\cdot(\nabla h_0)_{|\mathrm{H}} = n\cdot\epsilon_{\mathrm{P}}^{-1}(\xi_0^2 k^2)(\nabla h_0)_{|\mathrm{C}},\ \text{H–C interface}, \tag{2.14}$$

$$n\cdot\epsilon_{\mathrm{P}}^{-1}(\xi_0^2 k^2)(\nabla h_0)_{|\mathrm{C}} = 0,\ \text{R–C interface}. \tag{2.15}$$

Noting further that h_0 is continuous across these interfaces, we apply (2.11), (2.12), (2.14) and (2.15) to discover that h_0 is a constant function $h_0 = \bar{h}$ outside the rods. From linearity, it follows that the h_0 field inside the rod can be written as $h_0 = \bar{h}m(\mathbf{y})$, where

$$-\Delta m = \epsilon_{\mathrm{r}}\xi_0^2 k^2 m,\ \text{in the rod}, \tag{2.16}$$

and $m = 1$ on the boundary of the rod. Define the function $g(\mathbf{y})$ to be 1 for $\mathbf{y}$ outside the rod and $g(\mathbf{y})$ to be $m(\mathbf{y})$ for $\mathbf{y}$ inside the rod; then $h_0(\mathbf{y})$ is defined up to a multiplicative constant $\bar{h}$ and is given by

$$h_0(\mathbf{y}) = \bar{h}g(\mathbf{y}). \tag{2.17}$$

Next, we determine h_1 exterior to the rods. On equating like powers of η, we find that

$$-\Delta h_1 = 0 \tag{2.18}$$

outside the rods, and the corresponding transmission conditions for h_1 are given by

$$n \cdot \left(\nabla h_1 + \mathrm{i}\hat{\kappa}\bar{h}\right)_{|\mathrm{H}} = n \cdot \epsilon_{\mathrm{P}}^{-1}(\xi_0^2 k^2)\left(\nabla h_1 + \mathrm{i}\hat{\kappa}\bar{h}\right)_{|\mathrm{C}}, \text{ H–C interface,} \tag{2.19}$$

$$n \cdot \epsilon_{\mathrm{P}}^{-1}(\xi_0^2 k^2)\left(\nabla h_1 + \mathrm{i}\hat{\kappa}\bar{h}\right)_{|\mathrm{C}} = 0, \text{ R–C interface.} \tag{2.20}$$

Equation (2.18), transmission condition (2.19) and boundary condition (2.20) determine h_1 up to an additive constant c_1, and from the linearity of the problem we write $h_1 = \mathrm{i}\bar{h}W \cdot \hat{\kappa} + c_1$. Here, $W(\mathbf{y}) = (w_1(\mathbf{y}), w_2(\mathbf{y}))$, where w_i, $i = 1, 2$, are the periodic solutions of the cell problem

$$-\Delta w_i = 0, \text{ for } \mathbf{y} \text{ outside the rod,} \tag{2.21}$$

$$n \cdot \left(\nabla w_i + \mathrm{e}^{\mathrm{i}}\right)_{|\mathrm{H}} = n \cdot \epsilon_{\mathrm{P}}^{-1}(\xi_0^2 k^2)\left(\nabla w_i + \mathrm{e}^{\mathrm{i}}\right)_{|\mathrm{C}}, \text{ H–C interface,} \tag{2.22}$$

$$n \cdot \epsilon_{\mathrm{P}}^{-1}(\xi_0^2 k^2)\left(\nabla w_i + \mathrm{e}^{\mathrm{i}}\right)_{|\mathrm{C}} = 0, \text{ R–C interface,} \tag{2.23}$$

where $e^1 = (1, 0)$ and $e^2 = (0, 1)$. We define the region inside the period cell exterior to the rods by D and introduce the position-dependent dielectric constant $\epsilon(\mathbf{y})$, taking the value 1 inside the host and $\epsilon_{\mathrm{P}}(k^2\xi_0^2)$ inside the coating. For future reference, we introduce the tensor $\epsilon_{\mathrm{eff}}^{-1}(\xi_0^2 k^2)$ defined by

$$\epsilon_{\mathrm{eff}}^{-1}(\xi_0^2 k^2) = \int_D \epsilon(\mathbf{y})(\nabla W + I)\,\mathrm{d}\mathbf{y}, \tag{2.24}$$

where I is the 2×2 identity tensor.

Now we identify the effective magnetic permeability. Following [1] and [13], the average component of the B field parallel to the rods is given by

$$B_{\mathrm{ave}} = \frac{1}{d^2}\int_{Y_d} h(\mathbf{x})\,\mathrm{e}^{\mathrm{i}(k\hat{\kappa}\cdot\mathbf{x})}\mathrm{d}x_1\,\mathrm{d}x_2. \tag{2.25}$$

Here, Y_d is a period cell for the d-periodic crystal. Substituting the expansion (2.10) for h into (2.25), retaining the lowest-order terms and taking $d \to 0$ gives

$$\lim_{d\to 0} B_{\mathrm{ave}} = \bar{h}\int_Y g(\mathbf{y})\mathrm{d}y_1\,\mathrm{d}y_2. \tag{2.26}$$

The average component of the H field parallel to the rods is given by [1, 13]

$$H_{\mathrm{ave}} = \frac{1}{d}\int_{(0,0,0)}^{(0,0,d)} h(\mathbf{x})\,\mathrm{e}^{\mathrm{i}(k\hat{\kappa}\cdot\mathbf{x})}\mathrm{d}x_1\,\mathrm{d}x_2; \tag{2.27}$$

here the average is taken over any line parallel and exterior to the rods. Sending $d \to 0$ gives

$$\lim_{d\to 0} H_{\mathrm{ave}} = \bar{h}. \tag{2.28}$$

Using (2.26) and (2.28), the effective permittivity is given by

$$\lim_{d\to 0}\frac{B_{\mathrm{ave}}}{H_{\mathrm{ave}}} = \mu_{\mathrm{eff}}(\xi_0^2 k^2). \tag{2.29}$$

We recover the explicit form of the effective permeability $\mu_{\mathrm{eff}}(\xi_0^2 k^2)$ for a distribution of circular rods inside the unit period cell. To do so, recall the following Dirichlet eigenvalues E and eigenfunctions ψ for each rod cross section given by

$$-\Delta\psi = E\psi \quad \text{for } \mathbf{y} \text{ inside the rod} \quad \text{and} \quad \psi = 0 \quad \text{for } \mathbf{y} \text{ on the rod boundary.} \tag{2.30}$$

For rods with a circular cross-section of radius $0 < R_r < 1$ and polar coordinates $0 < \rho < R_r$, $0 \leqslant \theta < 2\pi$, let χ_{nm} be the mth zero of the nth Bessel function, then the Dirichlet eigenvalues are $E_{nm} = (\chi_{nm}/R_r)^2$, and the corresponding eigenfunctions are $\{J_n(\frac{\chi_{nm}}{R_r}\rho)\,e^{in\theta}, J_n(\frac{\chi_{nm}}{R_r}\rho)\,e^{-in\theta}\}$. The associated normalized eigenfunctions are denoted by $\psi^{\pm}_{nm}$. Note that the eigenvalue E_{0m} has only one associated normalized eigenfunction $\psi_{0m} = \frac{J_0(\chi_{0m}(\rho/R_r))}{\sqrt{\pi}R|J_0'(\chi_{0m})|}$ and $\langle\psi_{0m}\rangle^2 = \frac{4\pi R^2}{\chi^2_{0m}}$ when $n = 0$. Here, $\langle\cdot\rangle$ denotes the area integral over a rod cross-section. It is obvious that $\langle\psi^{\pm}_{nm}\rangle^2 = 0$ for $n \neq 0$.

Expanding $m(\mathbf{y})$ in the basis $\psi^{\pm}_{nm}$ noting that $m - 1 = 0$ outside the rods gives for each rod

$$m = 1 - \sum_{m=0}^{\infty} \frac{\xi_0^2 k^2}{\xi_0^2 k^2 - \frac{E_{0m}}{\epsilon_r}} \langle\psi_{0m}\rangle \psi_{0m}. \tag{2.31}$$

For a distribution of rods with radii R_{rj}, $j = 1, \ldots, \ell$, we have

$$\mu_{\text{eff}}(\xi_0^2 k^2) = \int_Y g(\mathbf{y})\,d\mathbf{y} = 1 - \sum_{j=0}^{\ell} N(R_{rj}) \sum_{m=0}^{\infty} \frac{4\pi R_{rj}^2}{\chi_{0m}^2} \frac{\xi_0^2 k^2}{\xi_0^2 k^2 - k_{jm}^2}, \tag{2.32}$$

where $N(R_{rj})$ is the number of rods with radius R_{rj} and $k_{jm}^2 = \frac{\chi_{0m}^2}{\epsilon_r R_{rj}^2}$.

Last, we find the homogenized subwavelength dispersion relation. Recall that $\xi^2 k^2 = \frac{\omega^2}{c^2}$ and from (2.10)

$$\frac{\omega^2}{c^2} = \frac{\omega_0^2}{c^2} + \eta \frac{\omega_1^2}{c^2} + \eta^2 \frac{\omega_2^2}{c^2} + \cdots, \tag{2.33}$$

where

$$\frac{\omega_i^2}{c^2} = \xi_i^2 k^2, \text{ for } i = 0, 1, \ldots. \tag{2.34}$$

The subwavelength dispersion relation is identified as the dispersion relation between ω_0 and $k\hat{\kappa}$ given by $\frac{\omega_0^2}{c^2} = \xi_0^2 k^2$. We now recover this dispersion relation by deriving the formula for ξ_0^2. Equating like powers of η gives the following equations for h_2 exterior to the rods,

$$-\left(\Delta h_2 + 2i\eta\hat{\kappa}\cdot\nabla h_1 - \eta^2 \bar{h}\right) = \xi_0^2 \bar{h}, \text{ in the host,} \tag{2.35}$$

$$-\left(\Delta h_2 + 2i\eta\hat{\kappa}\cdot\nabla h_1 - \eta^2 \bar{h}\right) = \xi_0^2 \epsilon_P(\xi_0^2 k^2)\bar{h}, \text{ in the coating,} \tag{2.36}$$

and the transmission conditions

$$\left(\xi_0^2 k^2 - \frac{\omega_p^2}{c^2}\right) n \cdot \left(\nabla h_2 + i\hat{\kappa} h_1\right)_{|H} + \left(\xi_1^2 k^2\right) n \cdot \left(\nabla h_1 + i\hat{\kappa}\bar{h}\right)_{|H}$$
$$= \left(\xi_0^2 k^2\right) n \cdot \left(\nabla h_2 + i\hat{\kappa} h_1\right)_{|C} + \left(\xi_1^2 k^2\right) n \cdot \left(\nabla h_1 + i\hat{\kappa}\bar{h}\right)_{|C}, \text{ H–C interface,} \tag{2.37}$$

$$\left(\xi_0^2 k^2\right) n \cdot \left(\nabla h_2 + i\hat{\kappa} h_1\right)_{|C} + \left(\xi_1^2 k^2\right) n \cdot \left(\nabla h_1 + i\hat{\kappa}\bar{h}\right)_{|C} + \left(\xi_2^2 k^2\right) n \cdot \nabla h_{0|C}$$
$$= \frac{1}{k^2 \epsilon_r}\left(\xi_0^2 k^2 - \frac{\omega_p^2}{c^2}\right) n \cdot \nabla h_{0|R}, \text{ R–C interface.} \tag{2.38}$$

Integrating and adding (2.35) and (2.36) gives the solvability condition

$$\xi_0^2 \int_D \bar{h}\,\mathrm{d}\mathbf{y} = -\int_{\mathrm{H}} \left(\Delta h_2 + 2\mathrm{i}\hat{\kappa}\cdot\nabla h_1 - \bar{h}\right)\mathrm{d}\mathbf{y} - \int_{\mathrm{P}} \epsilon^{-1}(\xi_0^2 k^2)\left(\Delta h_2 + 2\mathrm{i}\hat{\kappa}\cdot\nabla h_1 - \bar{h}\right)\mathrm{d}\mathbf{y}. \tag{2.39}$$

Integrating by parts and applying (2.13) together with the transmission conditions (2.15), (2.19), (2.20), (2.37) and (2.38) shows that (2.39) is equivalent to

$$\xi_0^2 = \mu_{\mathrm{eff}}^{-1}(\xi_0^2 k^2)\epsilon_{\mathrm{eff}}^{-1}(\xi_0^2 k^2)\hat{\kappa}\cdot\hat{\kappa}. \tag{2.40}$$

Writing $\omega_0^2/c^2 = \xi_0^2 k^2$ and substituting into (2.40) delivers the homogenized subwavelength dispersion relation

$$\frac{\omega_0^2}{c^2} = n_{\mathrm{eff}}^{-2} k^2, \tag{2.41}$$

where the effective index of diffraction n_{eff}^2 is given by

$$n_{\mathrm{eff}}^2 = \mu_{\mathrm{eff}}\left(\frac{\omega_0^2}{c^2}\right)\left(\epsilon_{\mathrm{eff}}^{-1}\left(\frac{\omega_0^2}{c^2}\right)\hat{\kappa}\cdot\hat{\kappa}\right)^{-1}. \tag{2.42}$$

Applying (2.9) and collecting results shows that to lowest order the Bloch waves $H = h(\mathbf{x})\mathrm{e}^{\mathrm{i}(k\hat{\kappa}\cdot\mathbf{x}-t\omega)}$ inside the metamaterial crystal are given by the subwavelength expansion

$$H(\mathbf{x},t) = \left(\bar{h}g\left(\frac{\mathbf{x}}{d}\right) + \eta h_1\left(\frac{\mathbf{x}}{d}\right) + O\left(\eta^2\right)\right)\exp\mathrm{i}(k\hat{\kappa}\cdot\mathbf{x} - t\left(\omega_0 + \eta\omega_1 + O\left(\eta^2\right)\right). \tag{2.43}$$

In the subwavelength limit the spatial averages of H correspond to spatial averages of plane waves associated with a magnetically active effective medium. To see this, take any planar averaging domain S and pass to the $d \to 0$ limit in the average to get

$$\begin{aligned}\lim_{d\to 0}\frac{1}{\mathrm{Area}(S)}\int_S H(\mathbf{x},t)\,\mathrm{d}x_1\,\mathrm{d}x_2 &= \lim_{d\to 0}\frac{1}{\mathrm{Area}(S)}\int_S \bar{h}g\left(\frac{\mathbf{x}}{d}\right)\exp\mathrm{i}(k\hat{\kappa}\cdot\mathbf{x} - t\omega_0)\,\mathrm{d}x_1\,\mathrm{d}x_2 \\ &= \frac{1}{\mathrm{Area}(S)}\int_S \mu_{\mathrm{eff}}\bar{h}\,\exp\mathrm{i}(k\hat{\kappa}\cdot\mathbf{x} - t\omega_0)\,\mathrm{d}x_1\,\mathrm{d}x_2.\end{aligned} \tag{2.44}$$

In a similar way, taking averages over any interval $a < x_3 < b$ on any line parallel to the x_3 axis not intersecting the coated rods gives

$$\begin{aligned}\lim_{d\to 0}\frac{1}{b-a}\int_{(0,0,a)}^{(0,0,b)} H(\mathbf{x},t)\,\mathrm{d}x_3 &= \lim_{d\to 0}\frac{1}{b-a}\int_{(0,0,a)}^{(0,0,b)} \bar{h}g\left(\frac{\mathbf{x}}{d}\right)\exp\mathrm{i}(k\hat{\kappa}\cdot\mathbf{x} - t\omega_0)\,\mathrm{d}x_3 \\ &= \frac{1}{b-a}\int_{(0,0,a)}^{(0,0,b)} \bar{h}\exp\mathrm{i}(k\hat{\kappa}\cdot\mathbf{x} - t\omega_0)\,\mathrm{d}x_3.\end{aligned} \tag{2.45}$$

Thus, the appropriate averages of the plane waves $H_{\mathrm{hom}} = \bar{h}\exp\mathrm{i}(k\hat{\kappa}\cdot\mathbf{x} - t\omega_0)$ and $B_{\mathrm{hom}} = \mu_{\mathrm{eff}}\bar{h}\exp\mathrm{i}(k\hat{\kappa}\cdot\mathbf{x} - t\omega_0)$ provide approximations to the average field seen in the d periodic metamaterial crystal for $0 < d \ll k$.

3. Electromagnetic fields inside coated rod assemblages

Here we introduce a special class of metamaterial crystals made from coated rod assemblages and derive an explicit formula for the subwavelength dispersion relation (2.41). The formula shows how the band structure depends explicitly on the distribution of rod radii, coating

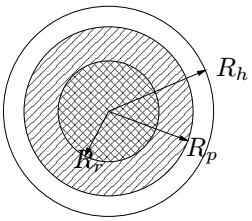

Figure 3. Doubly coated cylinder.

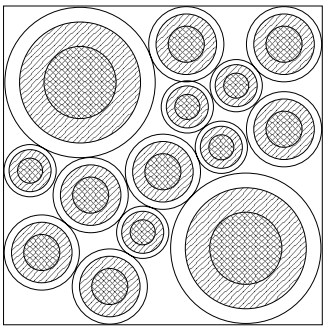

Figure 4. Cross-section of the unit period filled with coated rods. The coated rods fill all the space.

thickness and distance between neighboring rods. The assemblage is described as follows. Consider first the unit period cell Y filled with discs with radii ranging down to the infinitesimal. Inside each disc we place a centered rod cross-section, then a concentric coating of plasmonic material and finally a concentric coating of host material (see figure 3).

The cross sections of the coated rods together with the connected host material are depicted in figure 4. The ratio of the radii of the rod cross-section, plasmonic coating and host coating is the same for all the discs and we denote the area fractions of the host, coating and core phases by θ_{H}, θ_{P} and θ_{R}, respectively (see figure 3). The radii of the rods used in the assemblage are denoted by $R_{\mathrm{r}1} > R_{\mathrm{r}2} > R_{\mathrm{r}3} \cdots$. The number of rods having radius $R_{\mathrm{r}j}$ is denoted by $N(R_{\mathrm{r}j})$. For rods of radii $R_{\mathrm{r}j}$, the outer radius of the core is denoted by $R_{\mathrm{p}j}$, and the distance to the nearest-neighbor rod is $R_{\mathrm{h}j}$. For the coated rod assemblage it is clear that $R_{\mathrm{h}j}$ is determined by $R_{\mathrm{r}j}$ together with θ_{R} and θ_{P}.

This type of configuration is known in the composites literature and is referred to as a doubly coated cylinder assemblage [35]–[38].

The explicit formula for μ_{eff} follows from (2.32) and is given by

$$\mu_{\mathrm{eff}}\left(\frac{\omega_0^2}{c^2}\right) = 1 - \sum_{j=0}^{\infty} N(R_{\mathrm{r}j}) \sum_{m=0}^{\infty} \frac{4\pi R_{\mathrm{r}j}^2}{\chi_{0m}^2} \frac{(\omega_0/c)^2}{(\omega_0/c)^2 - k_{jm}^2}. \tag{3.1}$$

The poles of $\mu_{\mathrm{eff}}(\omega_0^2/c^2)$ are given by k_{jm}^2 (see figure 5).

The explicit formula for the effective dielectric permittivity follows from a standard calculation using (2.21), (2.22) and (2.23) (see for example [39]) and is given by

$$\epsilon_{\mathrm{eff}}^{-1} = \epsilon_{\mathrm{H}}^{-1} + \frac{2(1-\theta_{\mathrm{H}})\epsilon_{\mathrm{H}}^{-1}}{\theta_{\mathrm{H}} - \frac{2\epsilon_{\mathrm{H}}^{-1}}{\epsilon_{\mathrm{H}}^{-1} - \epsilon_{\mathrm{C}}^{-1}}} \tag{3.2}$$

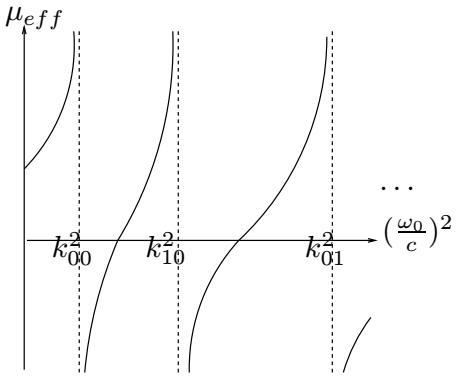

Figure 5. The relation between μ_{eff} and $(\omega_0/c)^2$.

with

$$\epsilon_{\text{C}}^{-1} = \epsilon_{\text{P}}^{-1} + \frac{2\theta_{\text{R}}\epsilon_{\text{P}}^{-1}}{2\theta_{\text{R}} - \theta_{\text{P}}}. \tag{3.3}$$

On writing $\epsilon_{\text{p}}(\omega_0^2/c^2) = 1 - \frac{\omega_{\text{p}}^2/c^2}{\omega_0^2/c^2}$ and $\epsilon_{\text{H}} = 1$, we obtain the formula for the frequency-dependent effective dielectric tensor given by

$$\epsilon_{\text{eff}}\left(\frac{\omega_0^2}{c^2}\right) = \frac{1-(\theta_{\text{R}}+\theta_{\text{P}})}{1+\theta_{\text{R}}+\theta_{\text{P}}} \left(\frac{\frac{1+\theta_{\text{R}}+\theta_{\text{P}}}{1-(\theta_{\text{R}}+\theta_{\text{P}})} + \left(1 - \frac{(\omega_{\text{p}}/c)^2}{(\omega_0/c)^2}\right)^{-1} \left(\frac{\theta_{\text{P}}}{2\theta_{\text{R}}+\theta_{\text{P}}}\right)}{\frac{1-(\theta_{\text{R}}+\theta_{\text{P}})}{1+\theta_{\text{R}}+\theta_{\text{P}}} + \left(1 - \frac{(\omega_{\text{p}}/c)^2}{(\omega_0/c)^2}\right)^{-1} \left(\frac{\theta_{\text{P}}}{2\theta_{\text{R}}+\theta_{\text{P}}}\right)} \right). \tag{3.4}$$

The dependence of μ_{eff} and ϵ_{eff} on the rod diameter and coating thickness and host area fraction is explicitly given by (3.1) and (3.4). This explicit dependence allows for the tuning of the dispersion relation

$$k^2 = \frac{\omega_0^2}{c^2} n_{\text{eff}}^2, \tag{3.5}$$

where

$$n_{\text{eff}}^2 = \mu_{\text{eff}}\left(\frac{\omega_0^2}{c^2}\right) \epsilon_{\text{eff}}\left(\frac{\omega_0^2}{c^2}\right). \tag{3.6}$$

For each coated rod with radius $R_{\text{r}j}$, outer coating radius $R_{\text{p}j}$ and nearest-neighbor distance $R_{\text{h}j}$, the field h_0 inside the rod is given by (2.31) and the field h_1 outside the rod is

$$h_1 = (1+\theta_{\text{R}})^{-1}\left(r\cos\gamma + \frac{R_{\text{r}j}^2}{r}\cos\gamma\right), \quad R_{\text{r}j} < r < R_{\text{p}j}, \tag{3.7}$$

$$\begin{aligned} h_1 = {} & \frac{2\theta_{\text{R}} + \theta_{\text{P}} + \theta_{\text{P}}\left(1 - \frac{\omega_{\text{p}}^2/c^2}{\omega_0^2/c^2}\right)^{-1}}{F} r\cos\gamma \\ & + \frac{2\theta_{\text{R}} + \theta_{\text{P}} - \theta_{\text{P}}\left(1 - \frac{\omega_{\text{p}}^2/c^2}{\omega_0^2/c^2}\right)^{-1}}{F} \frac{R_{\text{p}j}^2}{r}\cos\gamma, \quad R_{\text{p}j} < r < R_{\text{h}j}, \end{aligned} \tag{3.8}$$

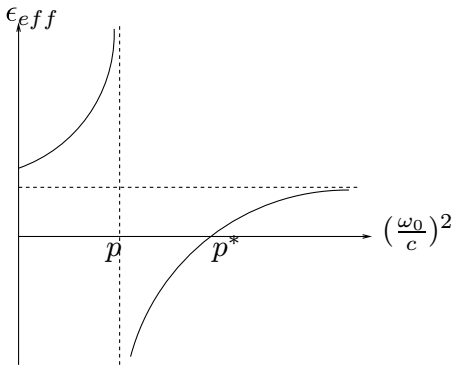

Figure 6. The relation between ϵ_{eff} and $(\omega_0/c)^2$.

where (r, γ) are local polar coordinates inside the coated rod and F is given by

$$F = (2\theta_{\text{R}} + \theta_{\text{P}})(1 + \theta_{\text{R}} + \theta_{\text{P}}) + \left(1 - \frac{\omega_{\text{p}}^2/c^2}{\omega_0^2/c^2}\right)^{-1} \theta_{\text{P}}(1 - (\theta_{\text{R}} + \theta_{\text{P}})). \tag{3.9}$$

It is clear that h_0 diverges inside the rods with radii $R_{\text{r}j}$ as ω_0^2/c^2 approaches k_{jm}^2, whereas h_1 diverges in the neighborhood of all the coated rods, $R_{\text{p}j} < r < R_{\text{h}j}$, as ω_0^2/c^2 approaches the zero of $\epsilon_{\text{eff}}\left(\frac{\omega_0^2}{c^2}\right)$.

4. Tunable double negative behavior

When ϵ_{eff} and μ_{eff} have the same sign, it is clear that $n_{\text{eff}}^2 > 0$ and wave propagation occurs. In this section, we show that it is possible to tune the assemblage through the choice of rod radii, coating thickness and host volume fraction to exhibit single negative, double negative and double positive behavior depending on the signs of ϵ_{eff} and μ_{eff}. For coated cylinder assemblages it is evident that the distance between neighboring rods and the coating thickness is explicitly determined by the area fraction of the host phase, the area fraction of the rods and the rod radii $R_{\text{r}j}$. The dielectric function (3.4) has only one pole and one zero, and these depend explicitly on the geometry of the coated rod assemblage and are given by

$$p = \left(\frac{\omega_{\text{p}}}{c}\right)^2 \frac{\theta_{\text{H}}(2\theta_{\text{R}} + \theta_{\text{P}})}{\theta_{\text{H}}(2\theta_{\text{R}} + \theta_{\text{P}}) + (2 - \theta_{\text{H}})\theta_{\text{P}}} \tag{4.1}$$

and

$$p^* = \left(\frac{\omega_{\text{p}}}{c}\right)^2 \frac{(2 - \theta_{\text{H}})(2\theta_{\text{R}} + \theta_{\text{P}})}{(2 - \theta_{\text{H}})(2\theta_{\text{R}} + \theta_{\text{P}}) + \theta_{\text{H}}\theta_{\text{P}}}. \tag{4.2}$$

Observe that $p < p^*$ and ϵ_{eff} is negative when $p < (\omega_0/c)^2 < p^*$. The relation between ϵ_{eff} and $(\omega_0/c)^2$ is displayed in figure 6.

From figures 5 and 6, it is clear that both ϵ_{eff} and μ_{eff} are negative for $p < (\omega_0/c)^2 < p^*$ provided that $(\omega_0/c)^2$ is simultaneously greater than but close to the poles of μ_{eff}. Therefore, for ϵ_{eff} and μ_{eff} to be simultaneously negative, it is required that $p < k_{jm}^2 < p^*$, i.e. the assemblage must contain rods with radii $R_{\text{r}j}$ satisfying the condition

$$\frac{\chi_{0m}^2 c^2}{\epsilon_{\text{r}}\omega_{\text{p}}^2} \frac{(2 - \theta_{\text{h}})(2\theta_{\text{r}} + \theta_{\text{p}}) + \theta_{\text{h}}\theta_{\text{p}}}{(2 - \theta_{\text{h}})(2\theta_{\text{r}} + \theta_{\text{p}})} < R_{\text{r}j}^2 < \frac{\chi_{0m}^2 c^2}{\epsilon_{\text{r}}\omega_{\text{p}}^2} \frac{\theta_{\text{h}}(2\theta_{\text{r}} + \theta_{\text{p}}) + (2 - \theta_{\text{h}})\theta_{\text{p}}}{\theta_{\text{h}}(2\theta_{\text{r}} + \theta_{\text{p}})}. \tag{4.3}$$

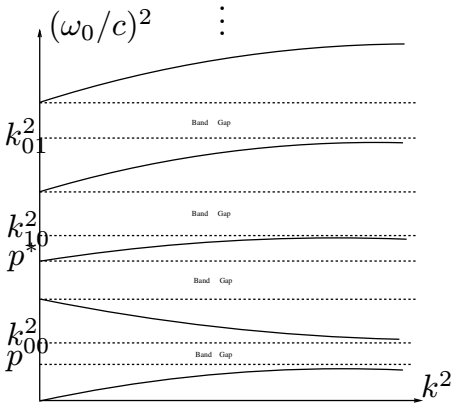

Figure 7. Dispersion relation $k^2 = (\frac{\omega_0}{c})^2 n_{\text{eff}}^2$ for a material with $\epsilon_{\text{p}} = 1 - \frac{\omega_{\text{p}}^2/c^2}{\omega_0^2/c^2}$, where $\omega_{\text{p}} = 25.8\,\text{THz}$. The assemblage contains rods of radii $R_{\text{r0}} = 0.2$ and $R_{\text{r1}} = 0.17$.

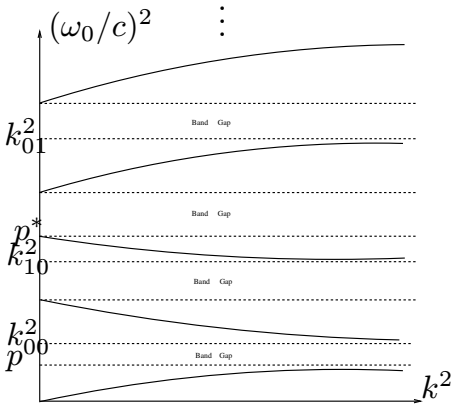

Figure 8. Dispersion relation $k^2 = (\frac{\omega_0}{c})^2 n_{\text{eff}}^2$ for a material with $\epsilon_{\text{p}} = 1 - \frac{\omega_{\text{p}}^2/c^2}{\omega_0^2/c^2}$, where $\omega_{\text{p}} = 25.8\,\text{THz}$. The largest two rod radii appearing in the assemblage are given by $R_{\text{r0}} = 0.2$ and $R_{\text{r1}} = 0.18$.

Now we fix the area fractions $\theta_{\text{R}} = 0.8$, $\theta_{\text{P}} = 0.1$, $\theta_{\text{H}} = 0.1$ and set $\omega_{\text{p}} = 25.8\,\text{THz}$ and $\epsilon_{\text{r}} = 200\,\text{m}^2$ so that $p = 0.349 \times 10^{10}\,\text{m}^{-2}$ and $p^* = 0.737 \times 10^{10}\,\text{m}^{-2}$. The dispersion relation $k^2 = (\frac{\omega}{c})^2 n_{\text{eff}}^2$ is displayed in figure 7 for an assemblage with the two largest rod radii chosen to be $R_{\text{r0}} = 0.2$ and $R_{\text{r1}} = 0.17$. These radii satisfy the requirement given by (4.3), while the radii of all other rods in the assemblage are chosen to lie below these two values and do not satisfy (4.3). It is clear from the figure that $\epsilon_{\text{eff}} < 0$ when $p < (\omega_0/c)^2 < p^*$ and otherwise $\epsilon_{\text{eff}} \geqslant 0$. In this example, p is below k_{00}^2 and p^* lies between k_{00}^2 and k_{10}^2. Note that in figure 7 the slope is negative for the dispersion curve lying between k_{00}^2 and p^*, indicating a negative group velocity.

In figure 8, we choose the largest two radii to be given by $R_{\text{r0}} = 0.2$ and $R_{\text{r1}} = 0.18$ and all other rods have radii below these values. For this case, p is below k_{00}^2 but p^* is between k_{10}^2 and k_{01}^2.

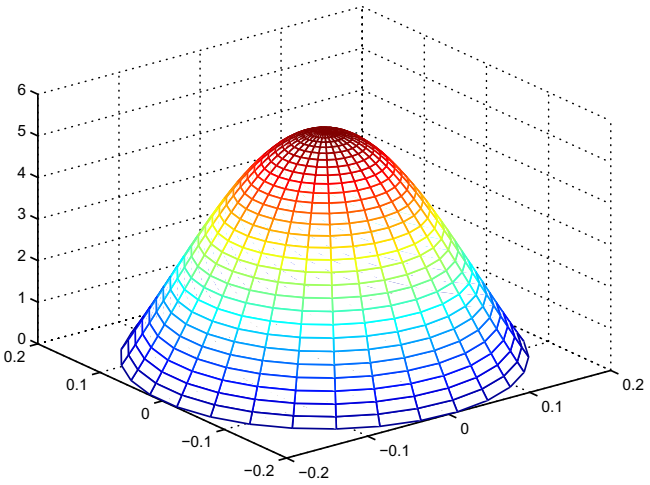

Figure 9. Graph of ψ_{00}.

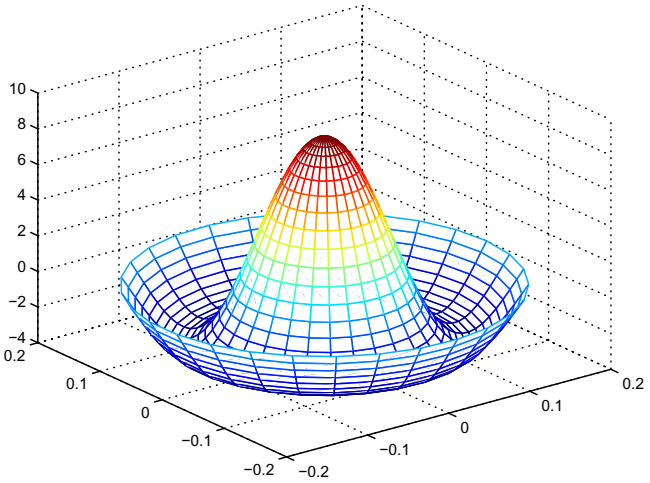

Figure 10. Graph of ψ_{01}.

Note that, for points $\mathbf{x}$ inside the coating phase and for $(\omega_0/c)^2$ close to k_{0m}^2, equations (2.31) and (2.43) show that $H(\mathbf{x}, t)$ behaves like $h(\mathbf{x})\mathrm{e}^{\mathrm{i}(k\hat{k}\cdot\mathbf{x}-t\omega)}$, where

$$h(\mathbf{x}) = \mu_{\mathrm{eff}}^{-1}\bar{h}\,\mathrm{e}^{\mathrm{i}k\hat{k}\cdot\mathbf{x}}\left(1 - \frac{(\omega_0/c)^2}{(\omega_0/c)^2 - k_{0m}^2}\langle 1|\psi_{0m}\rangle\right)\psi_{0m}. \tag{4.4}$$

In particular, when $(\omega_0/c)^2$ is near k_{00}^2, the profile of h is ψ_{00} (see figure 9 with $R_{\mathrm{r}0} = 0.2$) and when $(\omega_0/c)^2$ is near k_{01}^2, the profile of h is ψ_{01} (see figure 10 with $R_{\mathrm{r}0} = 0.2$).

Acknowledgments

This research was supported by NSF grant number DMS-0807265 and AFOSR grant number FA9550-05-0008.

References

[1] Pendry J, Holden A, Robbins D and Stewart W 1999 *IEEE Trans. Microw. Theory Tech.* **47** 2075–84
[2] Pendry J, Holden A, Robbins D and Stewart W 1998 *J. Phys.: Condens. Matter* **10** 4785–809
[3] Smith D, Padilla W, Vier D, Nemat-Nasser S and Schultz S 2000 *Phys. Rev. Lett.* **84** 4184–7
[4] Huangfu J, Ran L, Chen H, Zhang X, Chen K, Grzegorczyk T M and Kong J A 2004 *Appl. Phys. Lett.* **84** 1537
[5] Zhang F L, Potet S, Carbonell J, Lheurette E, Vanbesien O, Xiaopeng Z and Lippens D 2008 *IEEE Trans. Microw. Theory Tech.* **56** 2566
[6] Enkrich C, Wegener M, Linden S, Burger S, Zschiedrich L, Schmidt F, Zhou J F, Koschny T and Soukoulis C M 2005 *Phys. Rev. Lett.* **95** 203901
[7] Zhang S, Fan W, Minhas B K, Frauenglass A, Malloy K J and Brueck S R J 2005 *Phys. Rev. Lett.* **94** 037402
[8] Shalaev V M, Cai W, Chettiar U K, Yuan H K, Sarychev A K, Drachev V P and Kildishev A V 2005 *Opt. Lett.* **30** 3356–8
[9] Zhou X and Zhao X P 2007 *Appl. Phys. Lett.* **91** 181908
[10] Dolling G, Enrich C, Wegener M, Soukoulis C M and Linden S 2006 *Opt. Lett.* **31** 1800–2
[11] Jelinek L and Marques R 2010 *J. Phys.:Condens. Matter* **22** 025902
[12] Felbacq D, Guizal B, Bouchitte G and Bourel G 2009 *Microw. Opt. Technol. Lett.* **51** 2695–701
[13] O'Brien S and Pendry J B 2002 *J. Phys.: Condens. Matter* **14** 4035–44
[14] Lepetit T and Akmansoy E 2008 *Microw. Opt. Technol. Lett.* **50** 909–11
[15] Wheeler M S, Aitchison J S and Mojahedi M 2005 *Phys. Rev.* B **73** 045105
[16] Yannopapas V 2007 *Phys. Status Solidi (RRL)* **1** 208–10
[17] Yannopapas V 2007 *Appl. Phys. A: Mater. Sci. Process* **87** 259–64
[18] Figotin A and Kuchment P 1996 *SIAM J. Appl. Math.* **56** 68–88
[19] Figotin A and Kuchment P 1996 *SIAM J. Appl. Math.* **56** 1561–620
[20] Figotin A and Kuchment P 1998 *SIAM J. Appl. Math.* **58** 683–702
[21] Fortes S P, Lipton R P and Shipman S P 2010 *Proc. R. Soc.* A doi: 10.1098/rspa.2009.0542
[22] Fortes S P, Lipton R P and Shipman S P 2010 arXiv:1007.2640v1 [math-ph]
[23] Felbacq D and Bouchitte G 2005 *Phys. Rev. Lett.* **94** 183902
[24] Bouchitté G and Felbacq D 2005 *New J. Phys.* **7** 159
[25] Bouchitté G and Felbacq D 2004 *C. R. Acad. Sci., Paris* I **339** 377–82
[26] Zhikov V V 2004 *Algebra i Analiz* **16** 3458
Zhikov V V 2005 *St. Petersburg Math. J.* **16** 773790 (Engl. Transl.)
[27] Kohn R and Shipman S 2008 *SIAM Multiscale Model. Simul.* **7** 62–92
[28] Alu A and Engheta N 2008 *Phys. Rev.* B **78** 085112
[29] Tserkezis C, Papanikolaou N, Gantzounis G and Stefanou N 2008 *Phys. Rev.* B **78** 165114
[30] Bouchitté G and Schweizer B 2010 *SIAM J. Multiscale Model. Simul.* in preparation
[31] Chern R L and Felbacq D 2009 *Phys. Rev.* B **79** 075118
[32] Bouchitté G and Bourel C 2010 *Commun. Comput. Phys.* in preparation
[33] Farhat M, Guenneau, Enoch S and Movchan A B 2009 *Phys. Rev.* E **80** 046309
[34] Milton G W 2010 *New J. Phys.* **12** 033035
[35] Schulgasser K 1997 *Int. J. Heat Mass Transfer* **20** 1226–30
[36] Milton G W 1981 *Appl. Phys.* A **26** 125–30
[37] Lurie K A and Cherkaev A V 1985 *J. Optim. Theory Appl.* **46** 571–89
[38] Milgrom M 1989 *J. Appl. Phys.* **66** 3429–36
[39] Milton G W 2002 *The Theory of Composites* (Cambridge: Cambridge University Press)